5.1.6 Map of spatial distribution of the critical zones most prone to flood, extreme waves and seismic risks for HR test site

---

Final Version

Deliverable Number 5.1.6

Project Acronym	PMO-GATE
Project ID Number	10046122
Project Title	Preventing, Managing and Overcoming natural-hazards risk to mitiGATE economic and social impact
Priority Axis	2: Safety and Resilience
Specific objective	2.2: Increase the safety of the Programme area from natural and man-made disaster
Work Package Number	5
Work Package Title	Measures for risk mitigations
Activity Number	1
Activity Title	Improved early warning systems for single-hazard risk
Partner in Charge	UNIVERSITY OF FERRARA, DEPARTMENT OF ENGINEERING
Partners involved	UNIVERSITY OF SPLIT, FACULTY OF CIVIL ENGINEERING, ARCHITECTURE AND GEODESY
Status	Final
Distribution	Public

Summary

Abstract

This Deliverable presents visualization of spatial distribution of the critical zones most prone to flood, extreme sea waves and seismic action considered as single risks for the HR test site Kaštel Kambelovac, Croatian settlement located along the Adriatic coast. The visualization have been made through Geographic Information System (GIS) published as Web maps. Data in the maps for single risks are based on investigations of hazard, vulnerability and risk of the test site to floods, extreme sea waves and earthquakes. The maps enable to identify the buildings and areas with higher risk of natural disasters, which can be a very useful output for urban planning and management purposes. They give information about priorities to intervention to authorities and involved parties in HR test site in all phases of risk management.

1 Introduction

One of the purpose of PMO-GATE 5.1 Activity "Improved early warning systems for single risks" is creation of the maps of the spatial distribution of the critical zones most prone to flood, meteo-tsunami and seismic risk in a timely manner to give priority to intervention to authorities and involved parties in HR test site.

Namely, a more comprehensive understanding of the single risk results can be achieved by analysing their distribution over the test area. The use of the GIS tool makes it possible to spatially represent the global distribution of the hazard and vulnerability results, enabling the identification of buildings and areas with higher risk of natural disasters, which can be a very useful output for urban planning and management purposes.

The visualization of the spatial distribution of the data have been made through Geographic Information System (GIS) through the Web platform based on ESRI ArcGIS Online platform, which has been established for HR test site of the project. The Web platform has been used for visualization of the data for individual buildings, as well as for calculation and visualization of the critical zones prone to combined flood, extreme waves and seismic risk for HR test site.

Data in the maps for single risks are results of the investigations of hazard, vulnerability and risk of the test area to floods, extreme sea waves and earthquakes in WP3. The maps of flood hazard, seismic hazard, seismic vulnerability and seismic risk in terms of damage and in terms of peak ground accelerations have been made. The maps have been integrated into the GIS tool, wherein geo-referenced graphical data (vectorised information and orthophoto maps) were combined with building parameter information regarding the vulnerability and with hazard of the area for individual risks.

This document presents visualization of spatial distribution of the critical zones most prone to flood, extreme waves and seismic risk considered as single risks.

The maps are available at the site: https://pmo-gate.maps.arcgis.com/.

The *Home* page of the Web platform presents all important Web maps created in the project (Fig. 1). The Web maps have been created for the part of city of Kastela – Kastel Kambelovac – which represents HR test site of the PMO-GATE project.

Main characteristics:

Link: **https://pmo-gate.maps.arcgis.com/**

GIS platform: **ESRI ArcGIS Online**

Supported browsers: **Google Chrome, Microsoft Edge, Mozilla Firefox, Opera**

Supported devices: **PC, Tablet, Smartphone**

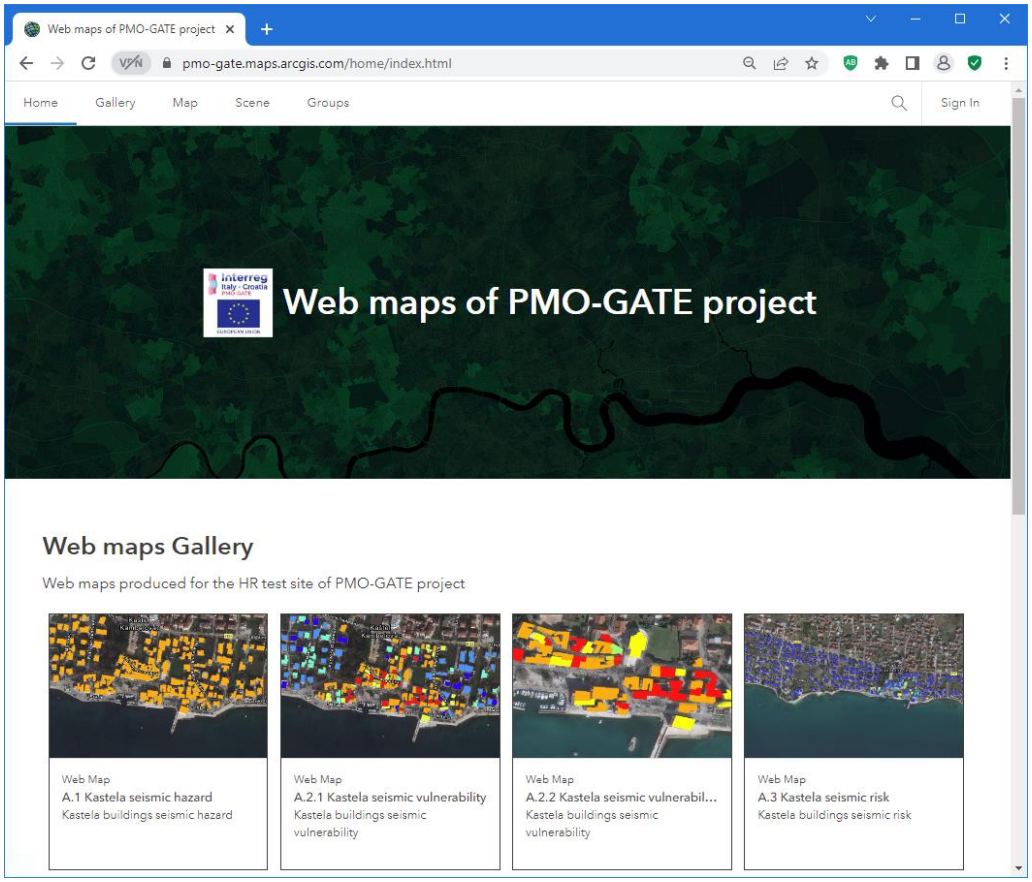

Fig. 1. Home page of the Web platform

There are three groups of Web maps, one group for each of potential natural-hazards in this area, with following enumeration:

A. Seismic,
B. Flood,
C. Extreme waves.

Furthermore, four types of maps for each natural-hazard are possible: hazard, vulnerability, risk and damage map. These maps have following enumeration:

1. Hazard map,
2. Vulnerability map,
3. Risk map,
4. Damage map.

Hazard and vulnerability maps have been created for all natural-hazards, but risk and damage maps have been made for seismic natural-hazard, only. In total, 11 maps have been made covering all type of maps and scenarios:

A.1	Kastela seismic hazard,
A.2.1	Kastela seismic vulnerability,
A.2.2	Kastela seismic vulnerability - historical center,
A.3	Kastela seismic risk,
A.4	Kastela seismic damage,
B.1.1	Kastela flood hazard - scenario 1 (yr 2046),
B.1.2	Kastela flood hazard - scenario 2 (yr 2065),
B.1.3	Kastela flood hazard - scenario 2 (yr 2100),
B.2	Kastela flood vulnerability,
C.1	Kastela extreme waves hazard,
C.2	Kastela extreme waves vulnerability.

These maps are valuable input for decision-makers and all other stakeholders, but they also represent an input for Multi-Hazard Risk Assessment based on Multi-Criteria Analysis that can be made on the two levels: buildings level and homogenous zones level.

2 Spatial distribution of the critical zones most prone to flood risks due to impact of climate changes on sea level rise

The spatial distribution of the area exposed to flood due to impact of climate changes on sea level rise and flood vulnerability indexes for the buildings that could be affected by flood are shown in this chapter. Data in the maps have been obtained through the investigations in Activity 3.1.

2.1 Spatial distribution of the critical zones most prone to flood

Spatial distribution of the exposure of the test site to flood is a result of analysis of sea level oscillations resulting from tidal effect, atmospheric pressure variations and climate change effect on sea level rise over the test area, given in Deliverable 3.1.2 [1]. Spatial distributions of critical zones most prone to flood risks for three scenarios (for years 2046, 2065 and 2100) are shown in Figs. 2-4 for the whole test site. Most exposed area is historical centre due to low-lying topography [2]. In addition, this area has significant number of cultural heritage and individual household objects located near the coastline. Therefore, Figs. 5-7 present the distribution of critical zones most prone to flood risks for the historical centre for the mentioned scenarios.

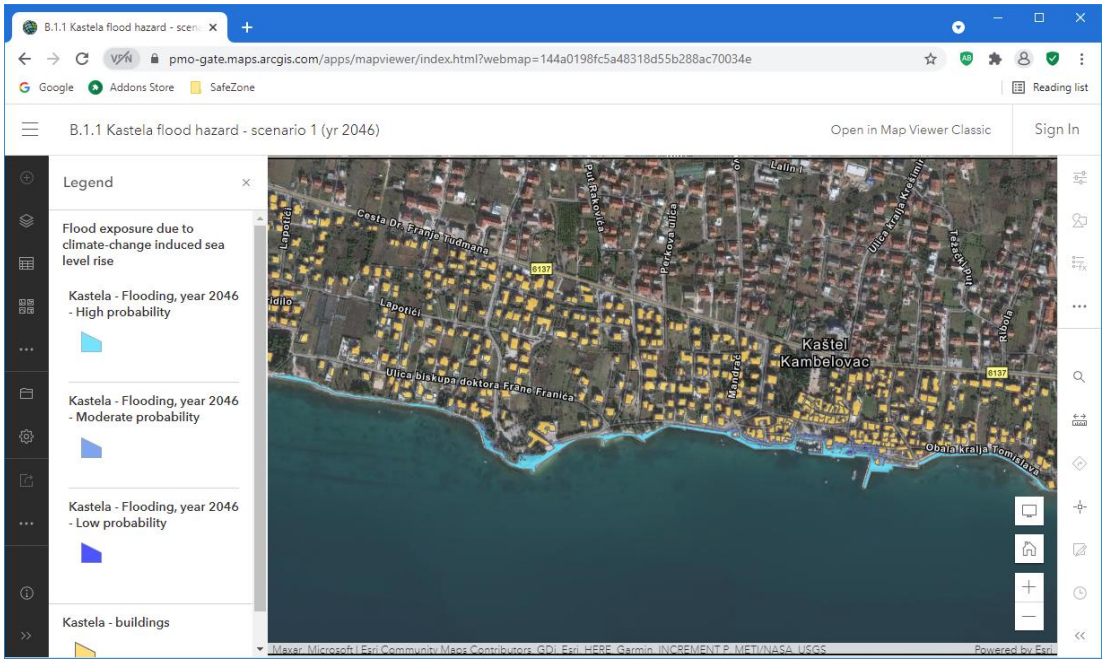

Fig. 2. Spatial distribution of critical zones most prone to flood due to impact of climate changes on sea level rise: scenario for year 2046 with respect to different probability

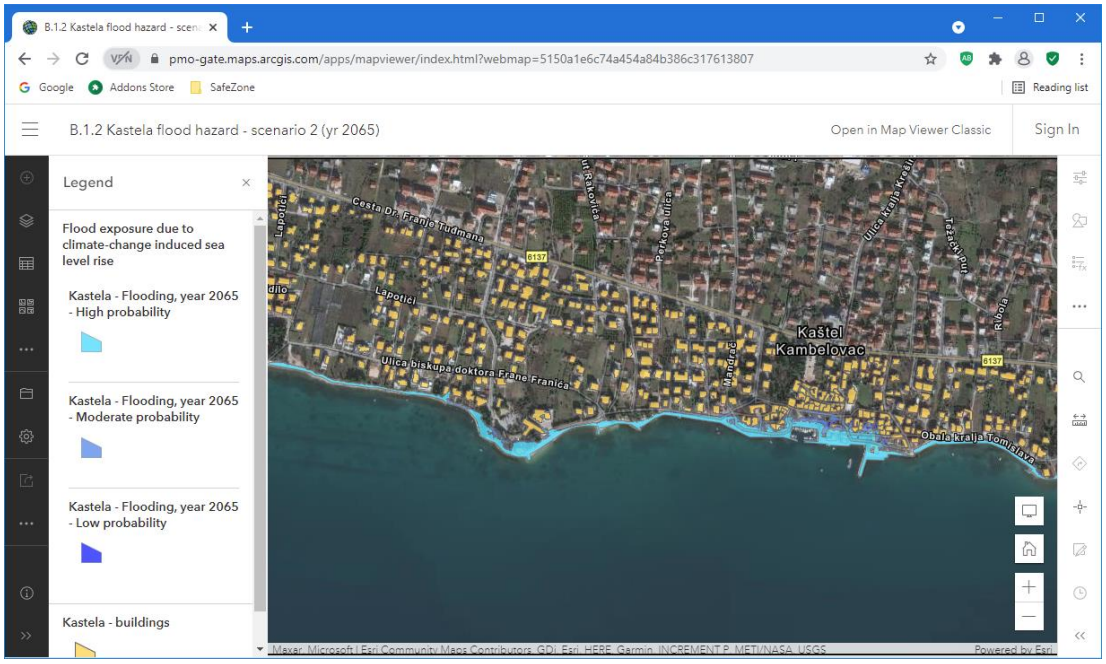

Fig. 3. Spatial distribution of critical zones most prone to flood due to impact of climate changes on sea level rise: scenario for year 2065 with respect to different probability

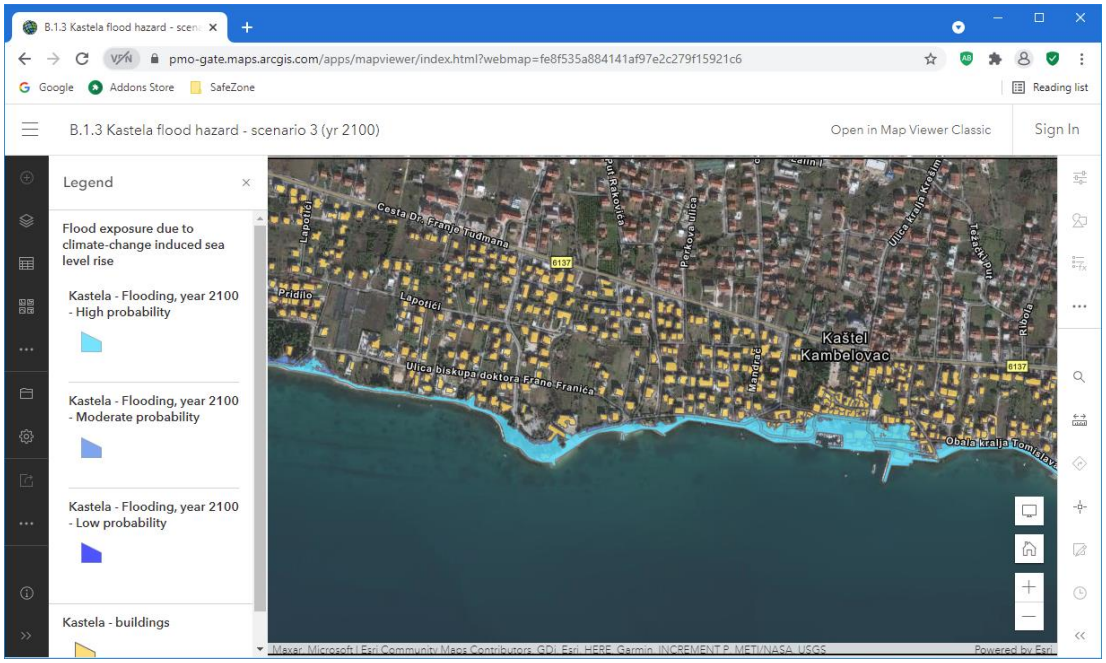

Fig. 4. Spatial distribution of critical zones most prone to flood due to impact of climate changes on sea level rise: scenario for year 2100 with respect to different probability

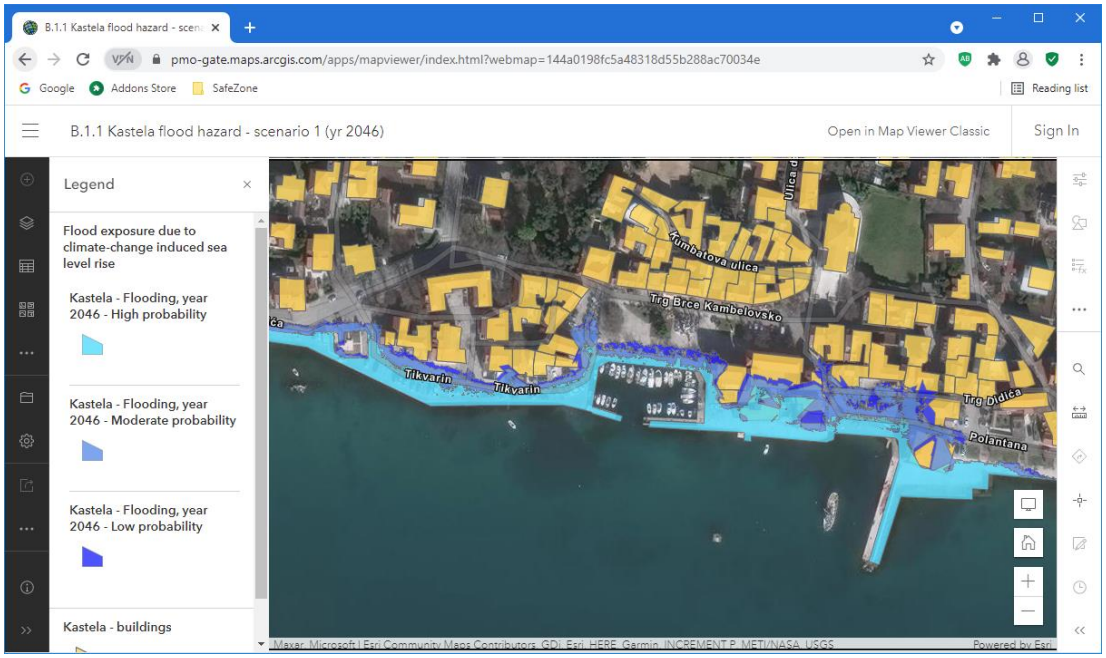

Fig. 5. Spatial distribution of critical zones most prone to flood risks due to impact of climate changes on sea level rise: scenario for year 2046 (historical centre)

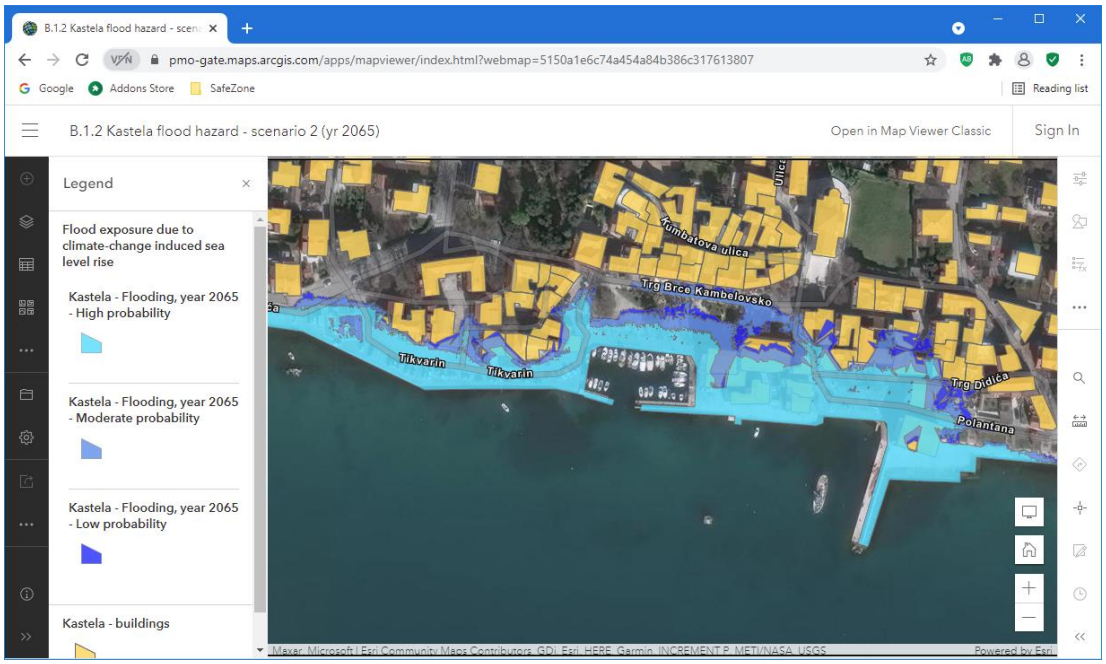

Fig. 6. Spatial distribution of critical zones most prone to flood risks due to impact of climate changes on sea level rise: scenario for year 2065 (historical centre)

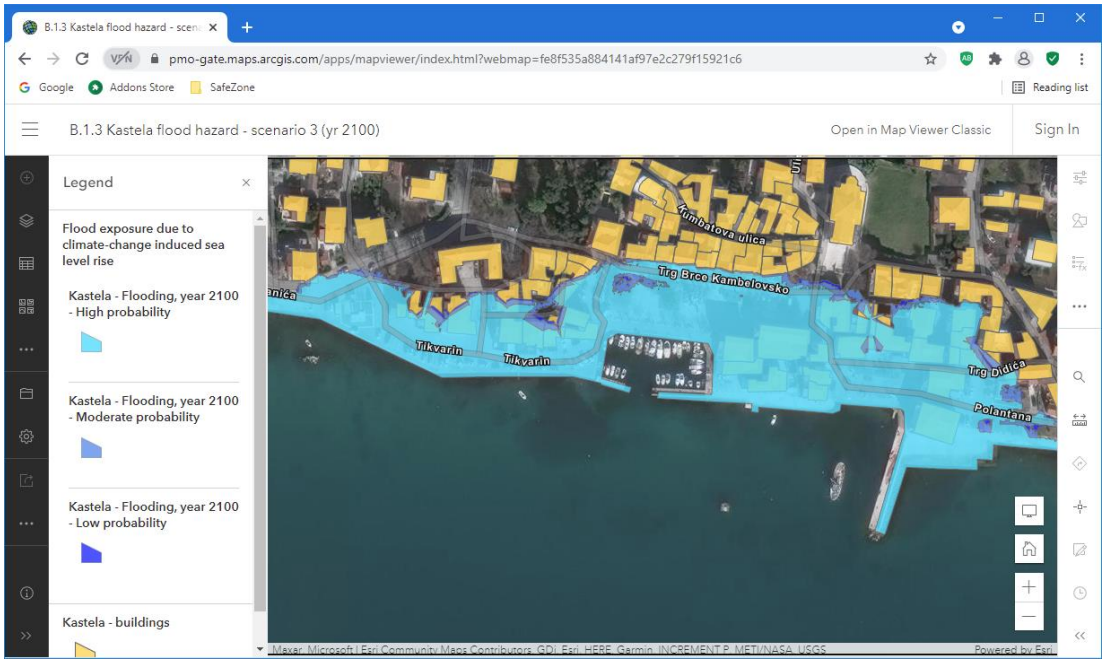

Fig. 7. Spatial distribution of critical zones most prone to flood risks due to impact of climate changes on sea level rise: scenario for year 2100 (historical centre)

2.2 Spatial distribution of the flood vulnerability in area exposed to floods

Distribution of the flood vulnerability indexes is given only for the buildings in the area exposed to floods. Calculation of flood vulnerability indexes is shown in Deliverable 3.1.3 [2]. It is shown in Fig. 8.

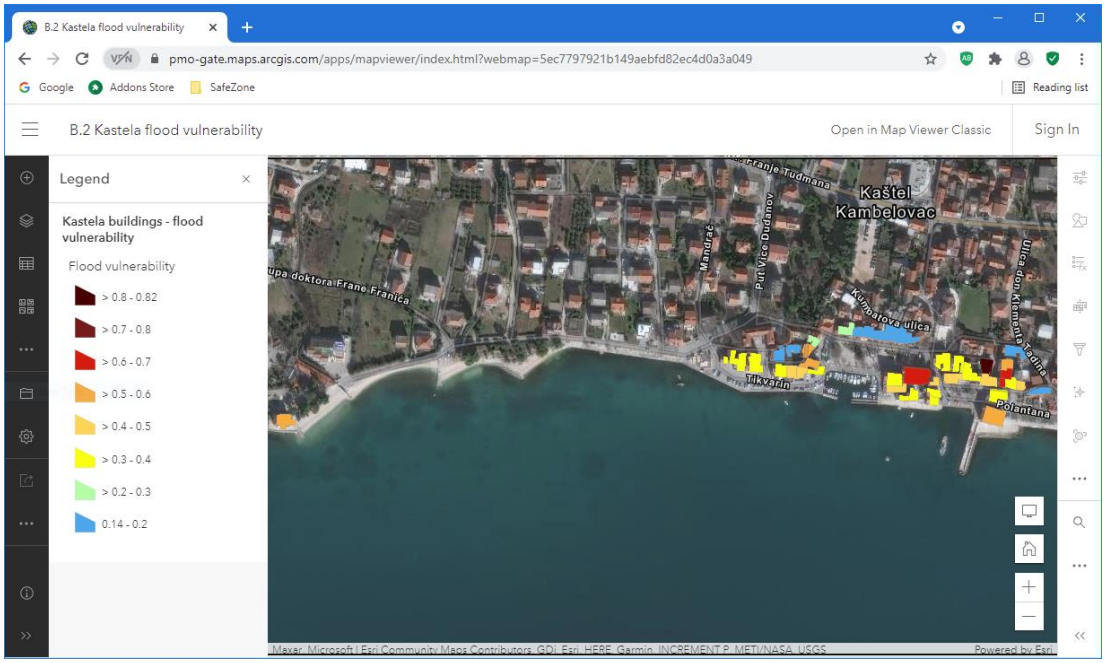

Fig. 8. Distribution of the flood vulnerability indexes in area exposed to floods

3 Spatial distribution of the critical zones most prone to the extreme sea waves exposure

The spatial distribution of the area exposed to the extreme sea waves and flood vulnerability indexes for the buildings that could be affected by extreme sea waves are shown in this chapter. Data in the maps have been obtained through the investigations in Activity 3.2.

3.1 Spatial distribution of the critical zones most prone to the extreme sea waves exposure

Spatial distribution of the critical zones most prone to the extreme sea waves exposure have been based on analysis of critical wind directions and velocities for extreme wave development and impact on HR pilot site. For selected wind scenarios wave development and transformation has been performed through extensive numerical modelling, resulting with different wave heights and inundation areas on the coastline (Deliverable 3.2.1 [3]). Using the data from wave scenarios and digital terrain model, vulnerability analysis of exposed objects has been performed using 'Extreme waves vulnerability index form' and resulting with main weak points of HR pilot site (Deliverable 3.2.2 [4]). The spatial distribution of the critical zones most prone to the extreme sea waves exposure is shown in Fig. 9. The extreme waves vulnerability map for the affected buildings is represented in Fig. 10.

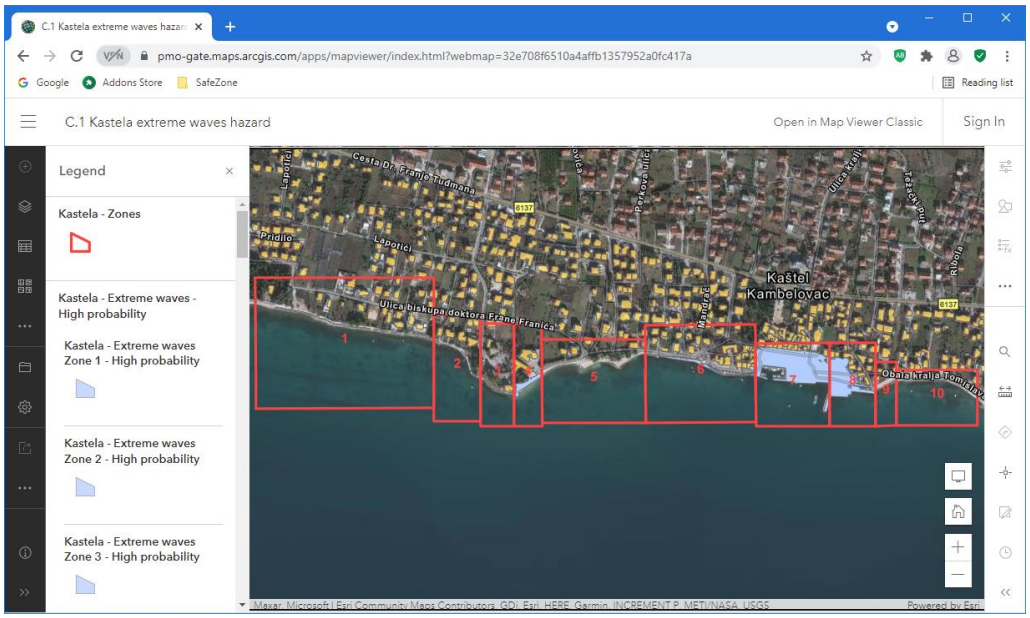

(a) Test site

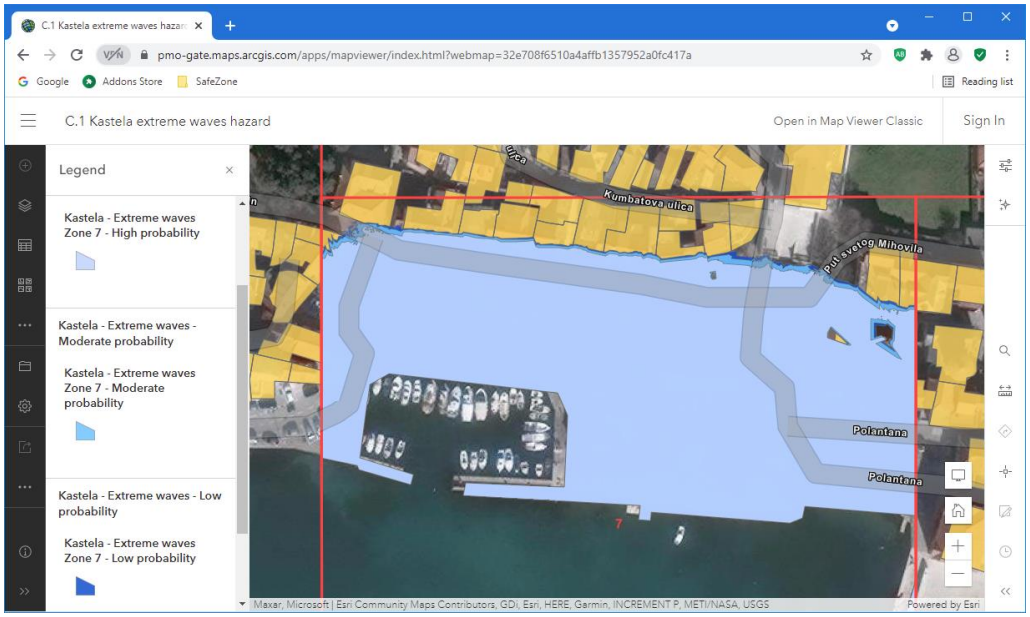

(b) Historical centre

Fig. 9. Spatial distribution of critical zones most prone to extreme sea waves exposure (historical centre)

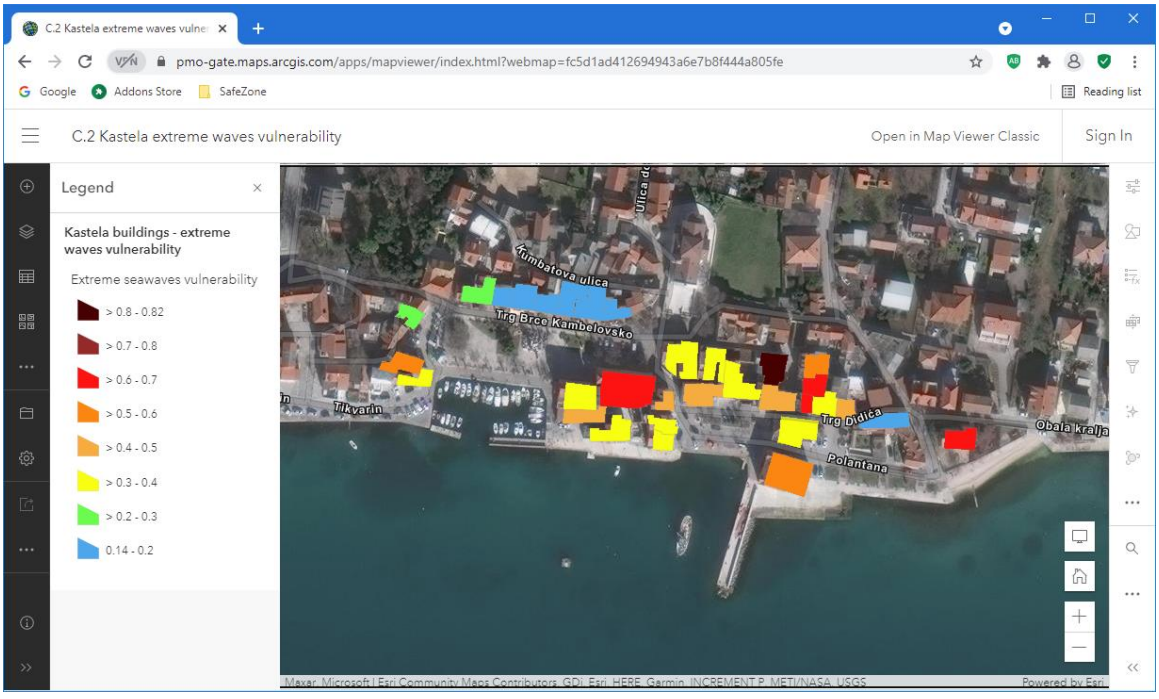

Fig. 10. Distribution of the extreme waves vulnerability indexes in area exposed to floods

4 Spatial distribution of the critical zones most prone to seismic risks

The spatial distribution of the seismic risks is a result of investigations of the hazard of test area, vulnerability indexes of the buildings, relations between vulnerability indexes and peak ground yield and capacity accelerations of the buildings and finally development of vulnerability curves for the buildings at the test site which give relationship between vulnerability indexes, demand peak ground accelerations for the chosen seismic scenarious and damage indexes of the buildings.

4.1 Spatial distribution of the seismic hazard

Distribution of seismic hazard in the test site have been defined according to seismic hazard map for Republic of Croatia [5]. In the Split and Kastela area, the seismic hazard is equal to a_g=0.22g for ground type A and return period T=475 years. Ground types A, B, C, D and E, may be used to account for the influence of local ground conditions on the seismic action. Geophysical investigation of a velocity of propagation of seismic waves based on travel time tomography of P, SV and SH arrivals acquired on three seismic lines on the shore of the Kaštela Bay indicateed the presence of shallow hard rock [6, 7], which can be clasified as soil type A (Deliverable 3.3.3 [8]). Considering these results and knowlege about ground properties from previous geotechnical investigations, the whole area have been taken to have type A ground. Thus, the seismic hazard for all buildings in the test area is same and it is equal to 0.22g for return period of 475 years.

Spatial distribution of the seismic hazard of the buildings over the test area is presented in Fig. 11.

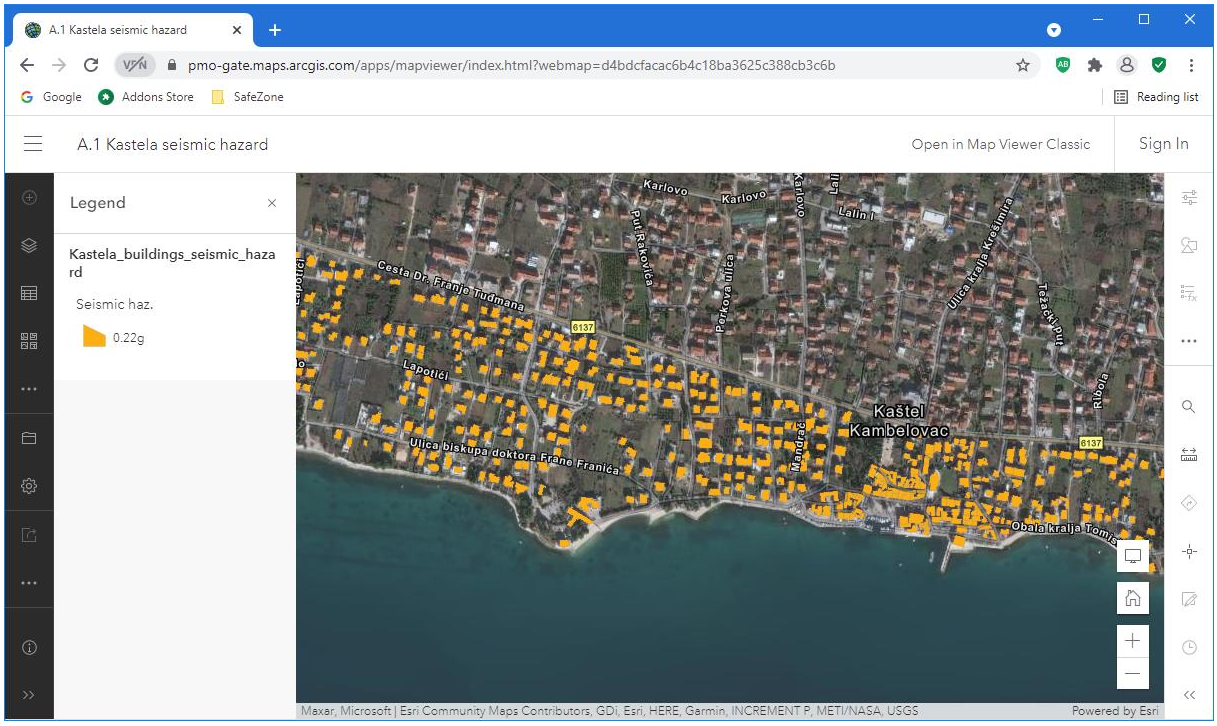

Fig. 11. Spatial distribution of the seismic hazard over the HR test area

4.2 Spatial distribution of the seismic vulnerability

Seismic vulnerability is measured by seismic vulnerability index of individual buildings. Vulnerability indexes for the buildings in HR test site (Deliverable 3.3.3 [8]) were calculated according the methodology presented in Deliverable 3.3.1 [9]. They are presented in the seismic vulnerability map of the test area, Deliverable 3.3.4 [10].

Spatial distribution of the seismic vulnerability indexes of the buildings over the test area is presented in Figs. 12 and 13.

Fig. 12 shows seismic vulnerability maps for the buildings in the test site where the buildings are divided into 4 vulnerability classes: Low vulnerability for $I_v<30$, Medium-low vulnerability for $30<I_v<45$, Medium-high vulnerability for $45< I_v<60$, High vulnerability for $I_v>60$. The highest vulnerability is achieved in historical centre were all buildings are made as stone masonry structures.

In the northern part, which does not belong to the protected historic core, there are a number of stone masonry buildings. Therefore, most of the buildings belong to High, Medium-High and Medium-Low vulnerability classes. Only two buildings have Low vulnerability class.

In the eastern and western parts of the test site, the buildings are built with concrete or clay blocks, without confinement, only with confinement horizontal tie beams or with horizontal and vertical confinement. They mostly belong to the low vulnerability class ($I_v<30\%$). Within this class, however, there are visible differences in vulnerability, which can be seen in Fig. 13. Newer buildings with clay blocks and horizontal and vertical confinement have generally the least vulnerability (less than 10%). Older buildings with concrete blocks and horizontal confinement have approximately index between 10% and 20%. Buildings without confinement or the previous one, but irregular in height and / or layout in plan with several appendices and additions, have an index mostly between 20% and 30%.

Both maps (Figs. 12 and 13) provides useful information for the crises management. They also provide an insight into the vulnerability of buildings in the test area and can optionally serve authorities to determine priorities in the reconstruction of buildings and improve their seismic resistance.

The second map (Fig. 13), made with distribution of the buildings into classes of 10%, gives more comprehensive insight into the building's vulnerability. Thus, it can be usefull both in crises managment and as information to owners of the buildings and city planers about vulnerability state of individual buildings.

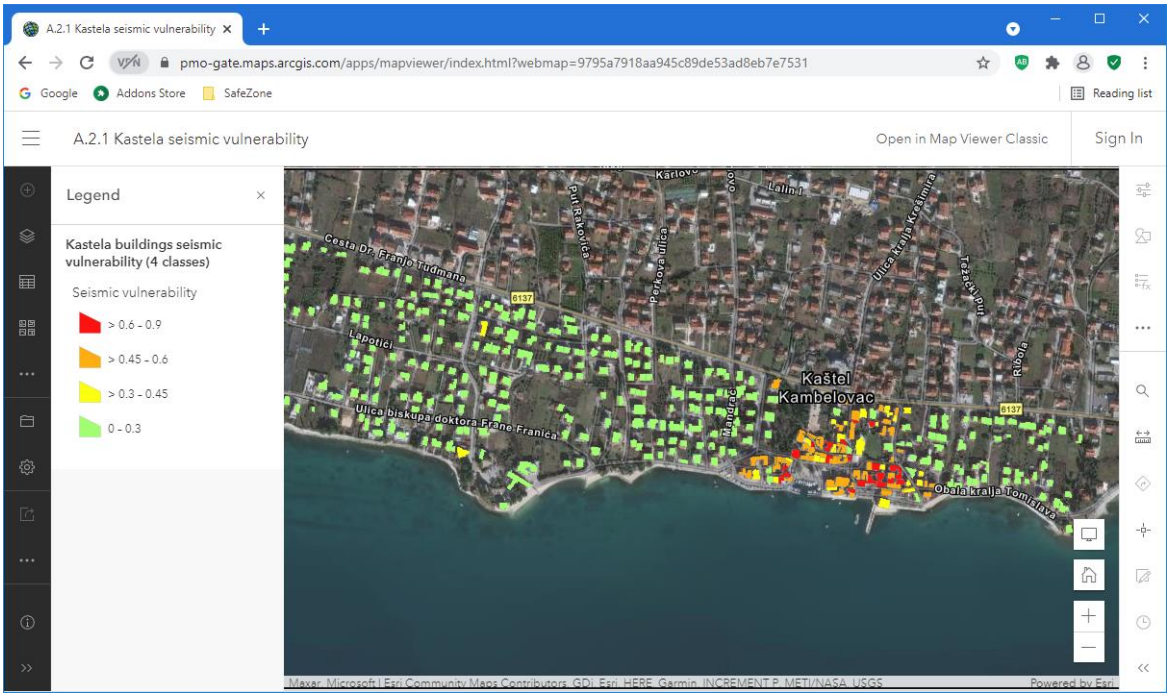

Fig. 12. Vulnerability of the buildings in the whole test site divided into 4 classes

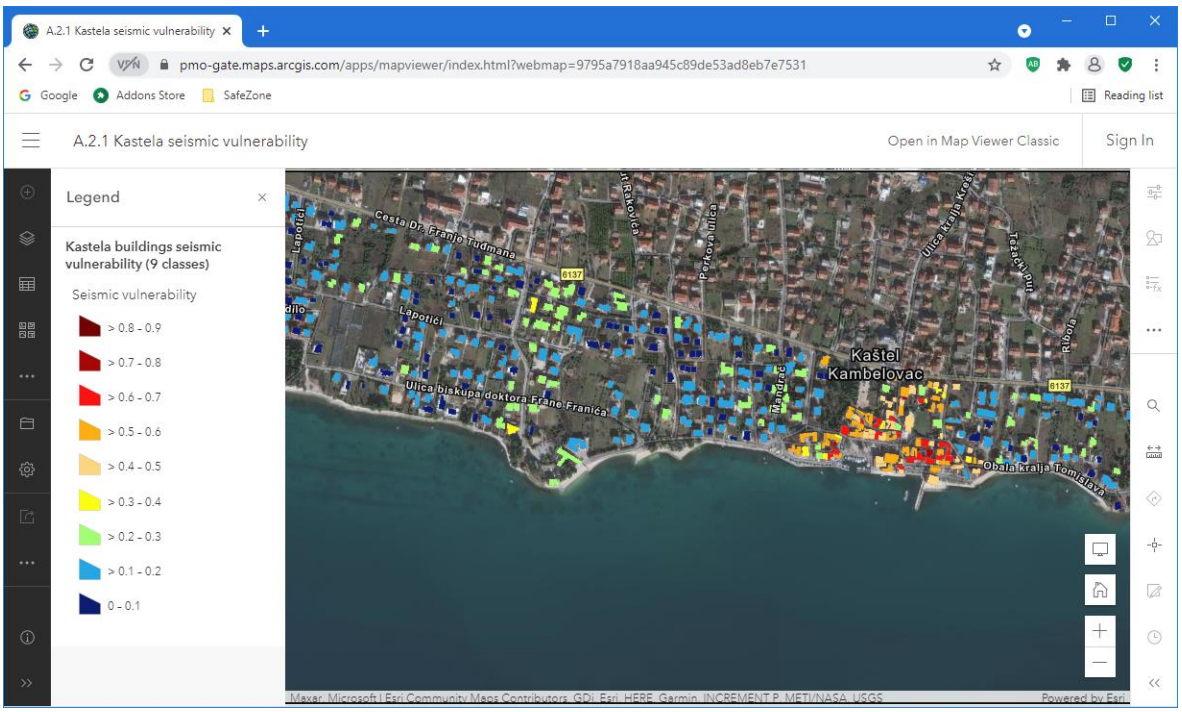

Fig. 13. Vulnerability of the buildings - division into classes of 10%

Both maps clearly show the difference between the vulnerability of the historical core and the area north of the core, where mostly stone masonry buildings were built from the 15th to the beginning of the 20th century, from the rest of the area where buildings are built of concrete and clay blocks, mostly after 1950. until today.

Web map also includes layers with the vulnerability indexes of the buildings in the historical centre together with the distribution of vulnerability parameters which constitute seismic vulnerability index (Figs. 14-15). These layers are of special importance to analyze the causes of high seismic vulnerability in the centre.

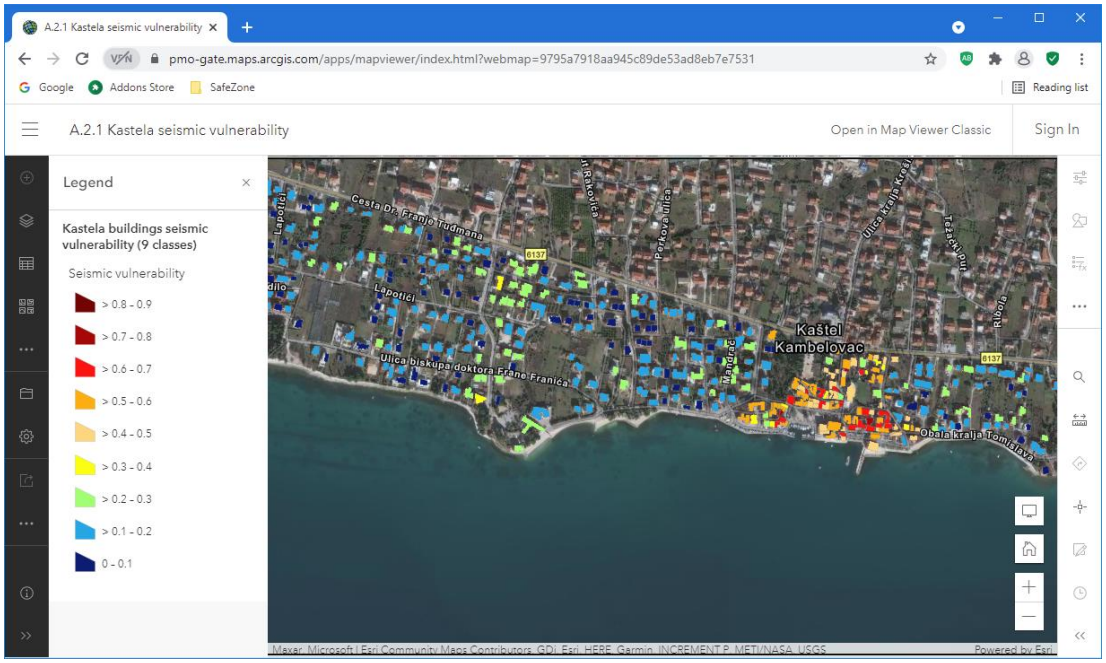

Fig. 14. Distribution of vulnerability indexes of the buildings in historical centre.

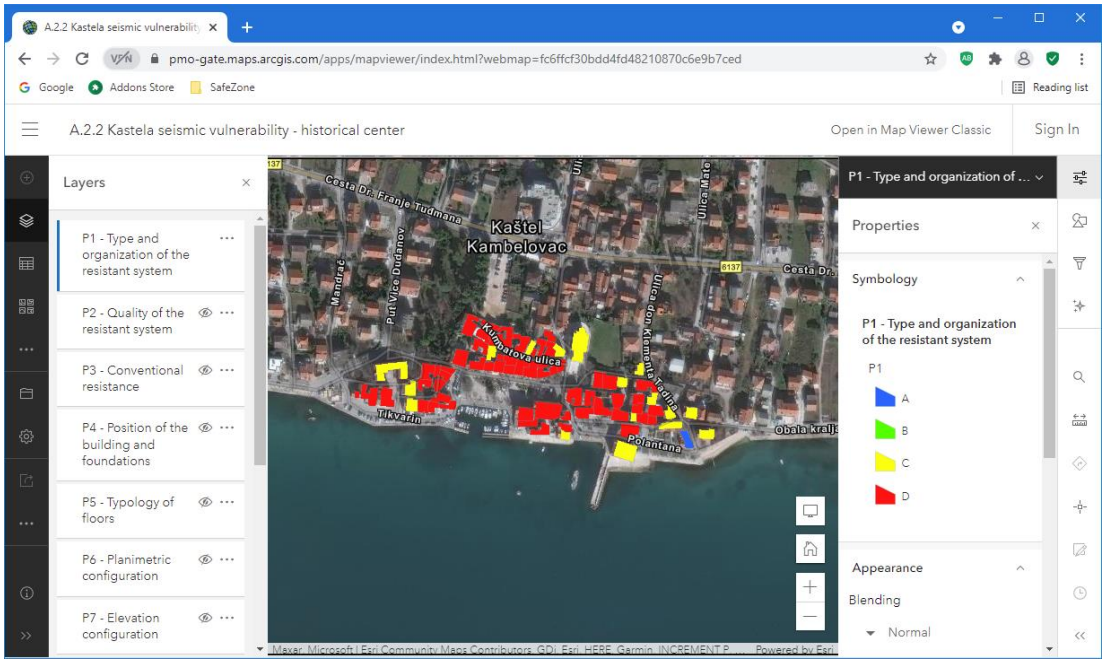

(a) P1 - Type and organization of the resistant system

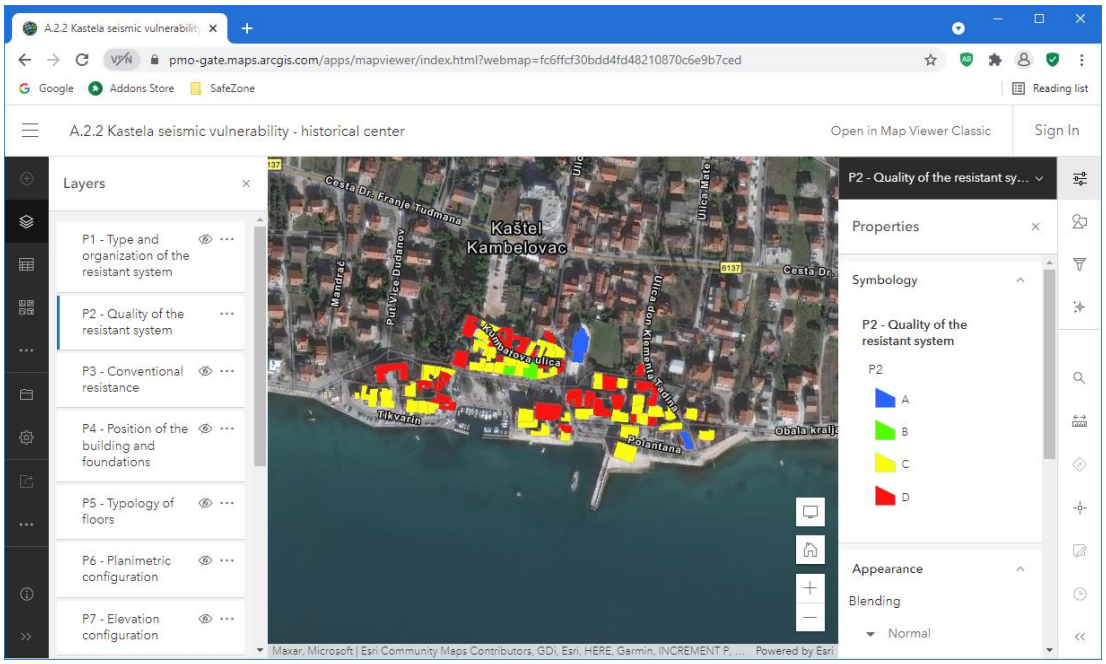

(b) P2 - Quality of the resistant system

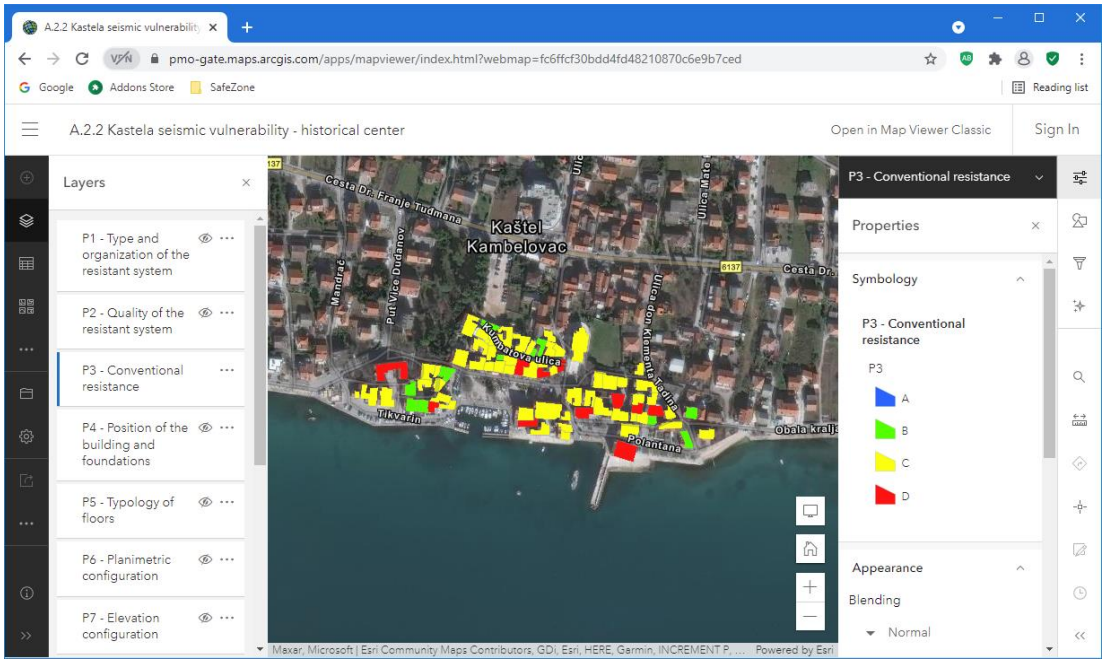

(c) P3 - Conventional resistance

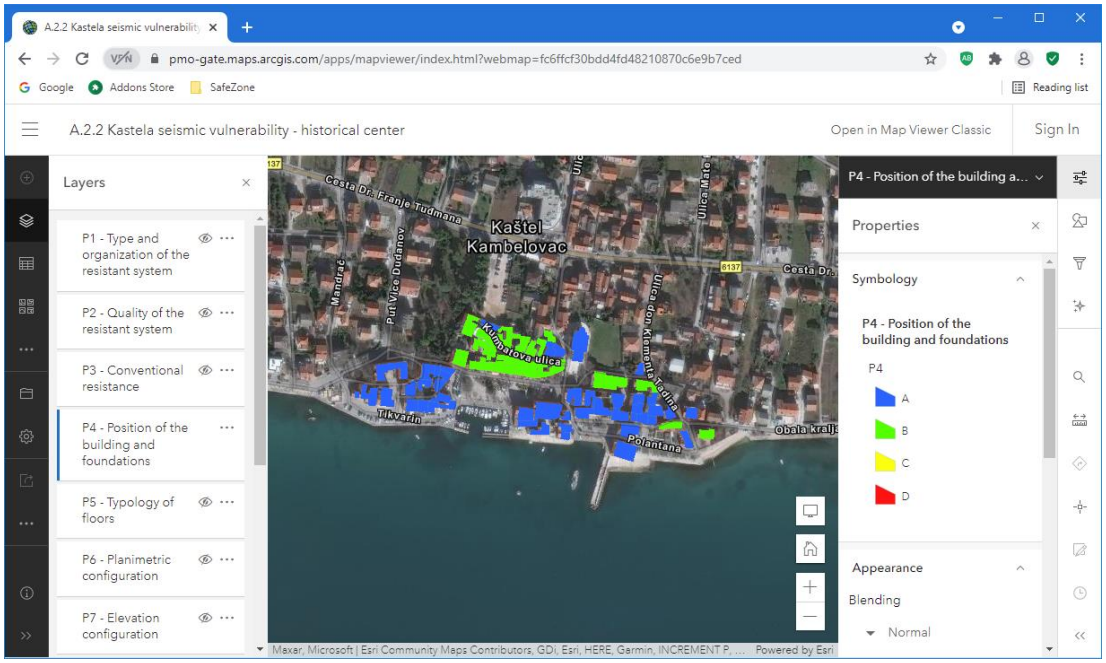

(d) P4 - Position of the buildings and foundations

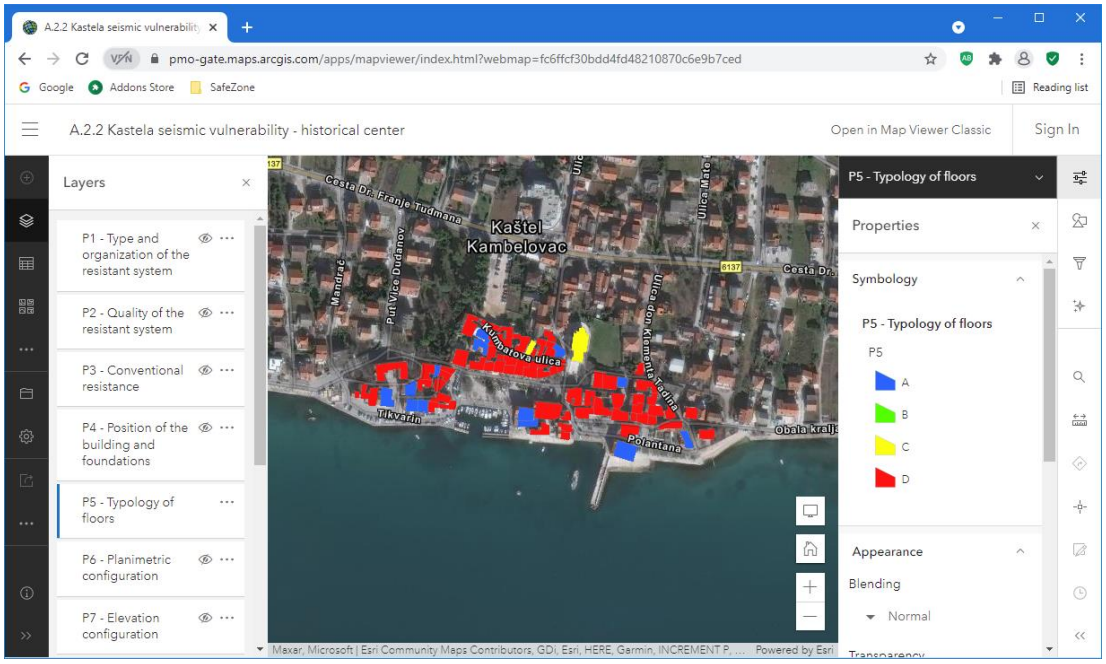

(e) P5 - Typology of floors

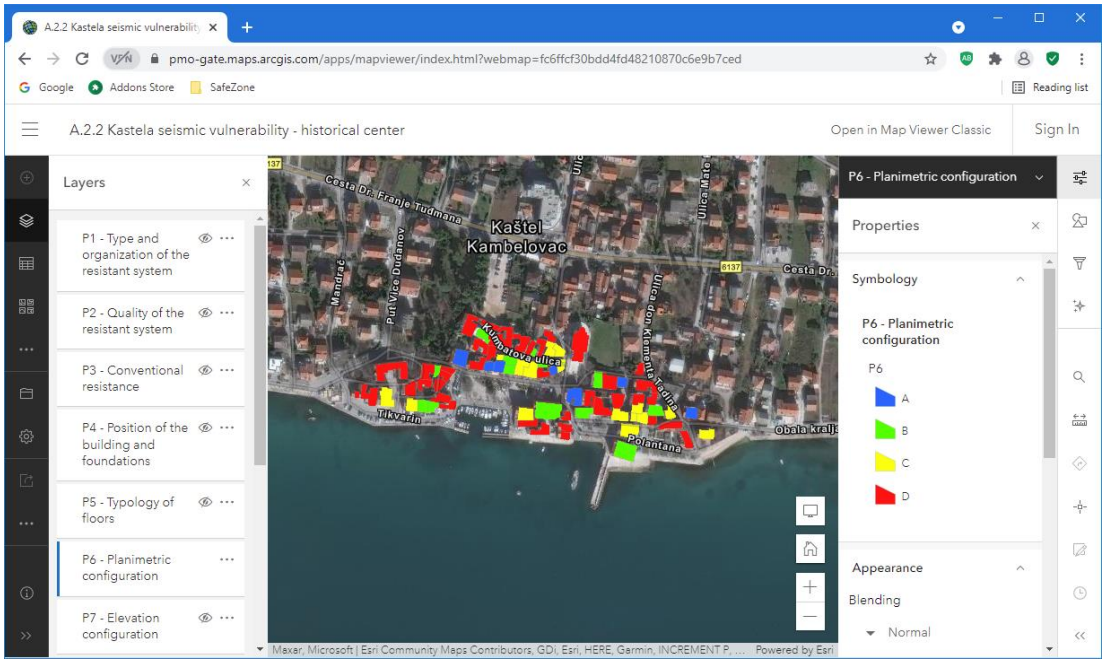

(f) P6 - Planimetric configuration

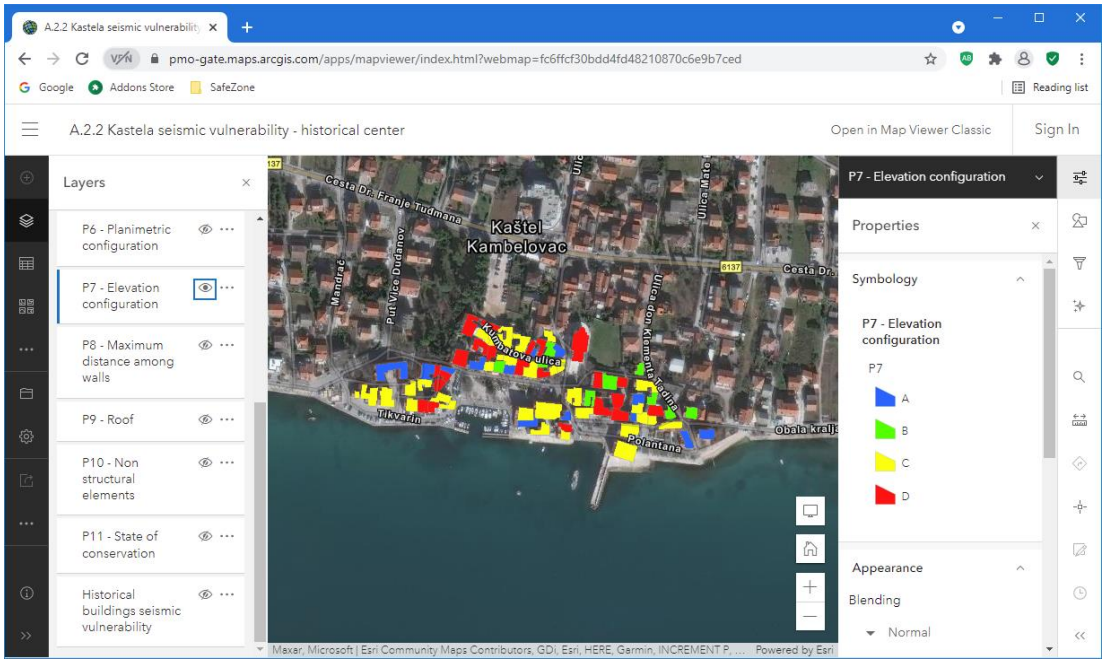

(g) P7 – Elevation configuration

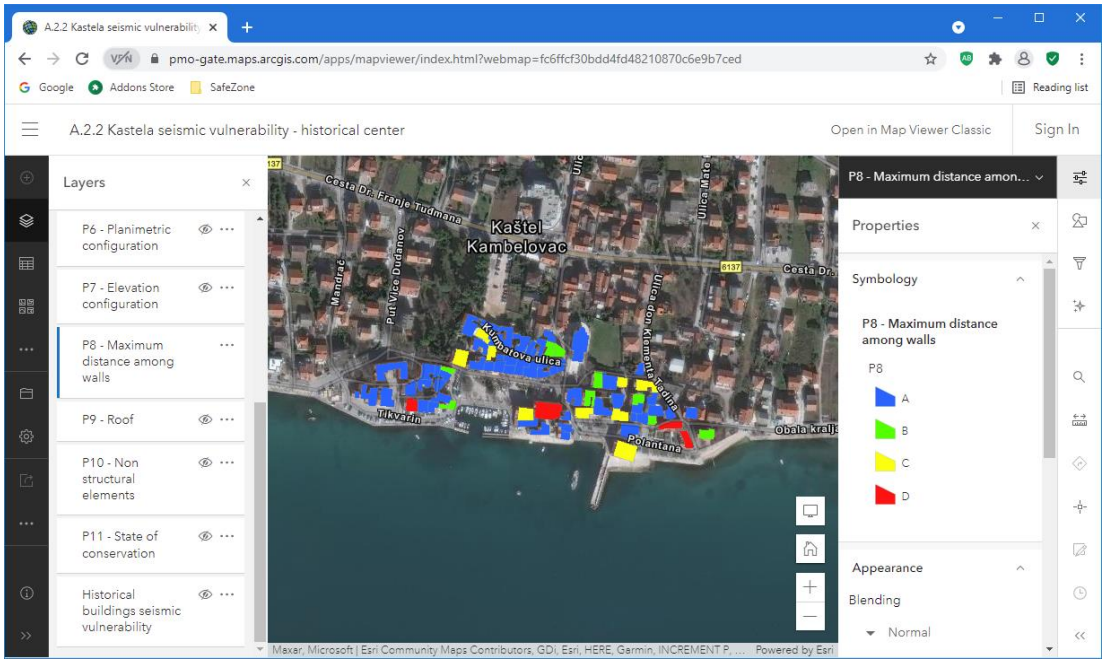

(h) P8 - Maximum distance among walls

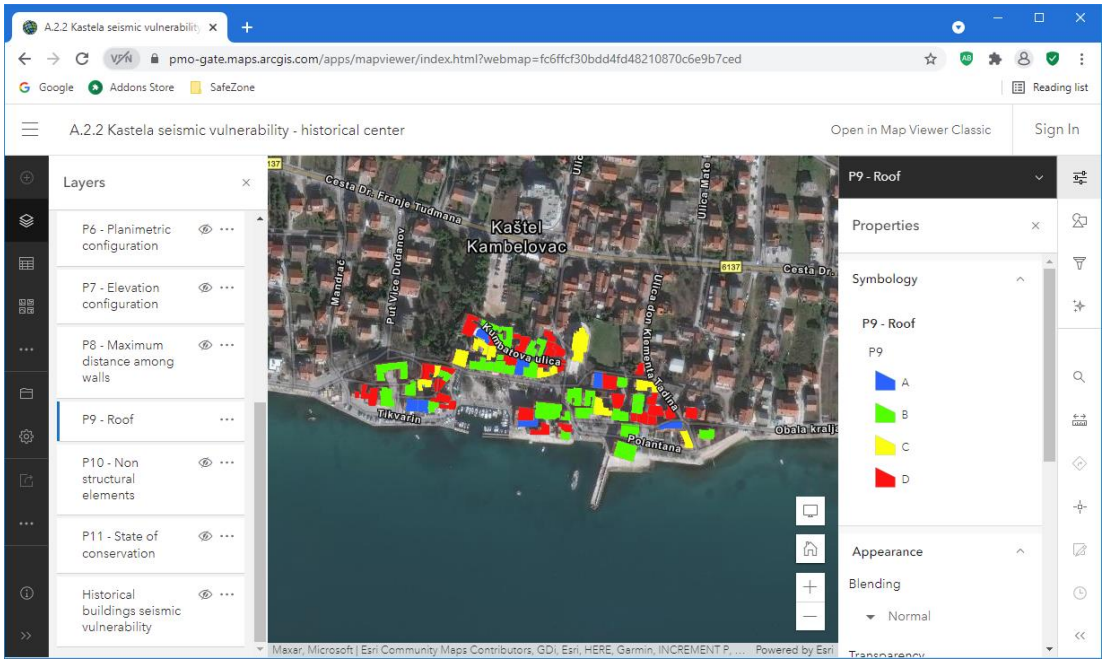

(i) P9 - Roof

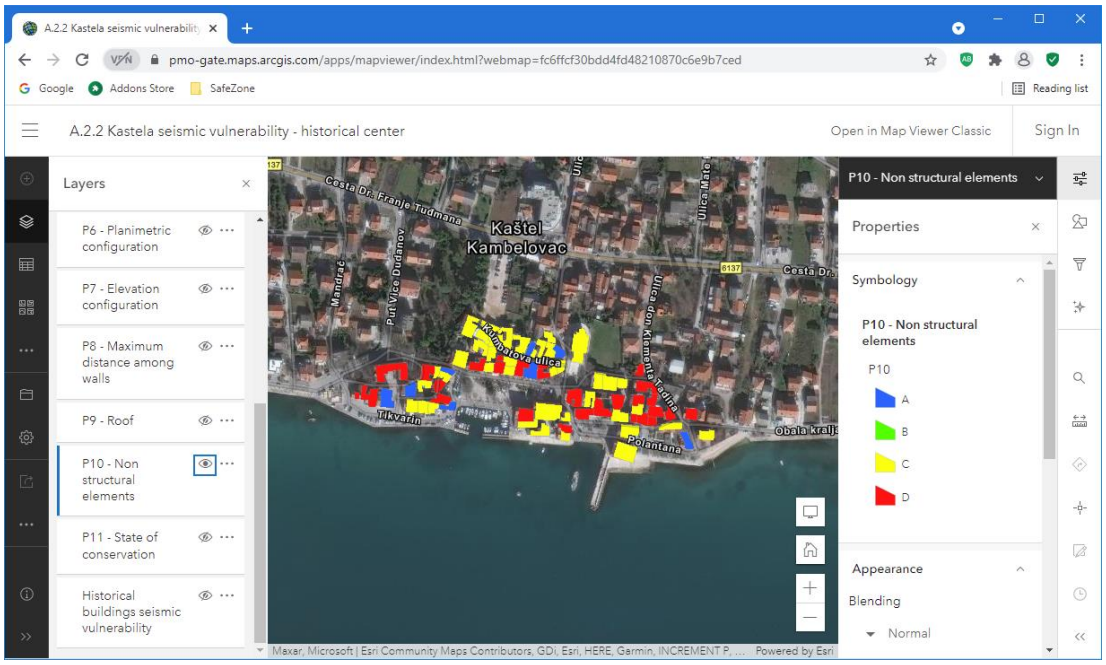

(j) P10 - Non structural elements

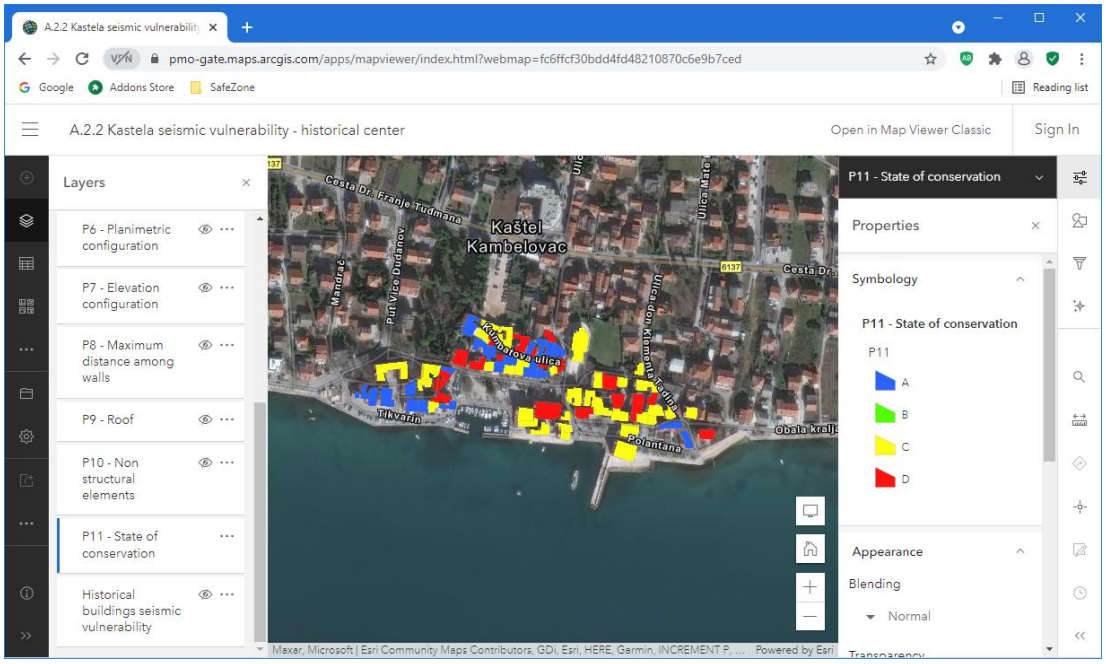

(k) P11 - State of conservation

Fig. 15. Distribution of the parameters of seismic vulnerability index in historical centre.

4.3 Spatial distribution of the seismic risk

Seismic risk can be considered as a function of seismic hazard and vulnerability. In this project, seismic risk is represented in terms of damage and peak ground accelerations of the buildings at the test site. It has been calculated according to methodology developed in WP3 of the project. Description of the methodology are given in an article [11] and Deliverables 3.3.1, 3.3.3 and 3.3.4 [8-10]. In this section the maps of the spatial distribution of the damage and indexes of seismic risk are presented.

4.3.1 Spatial distribution of the seismic risk in terms of damage

Spatial distribution of the seismic risk in terms of the damage is represented by the damage index maps of the investigated area for given intensity of the earthquake. Three seismic scenarious corresponding to return periods 95, 225 and 475 years and demand peak ground accelerations of 0.11g, 0.17g and 0.22g, respectively, have been chosen in this investigations (Fig. 16). The damage index is expressed in the 0–1 space by means of a tri-linear law defined by the yield acceleration, PGA_y (damage equal to 0), which represents the beginning of the damage, and the acceleration of the collapse of the building, PGA_c (damage equal to 1).

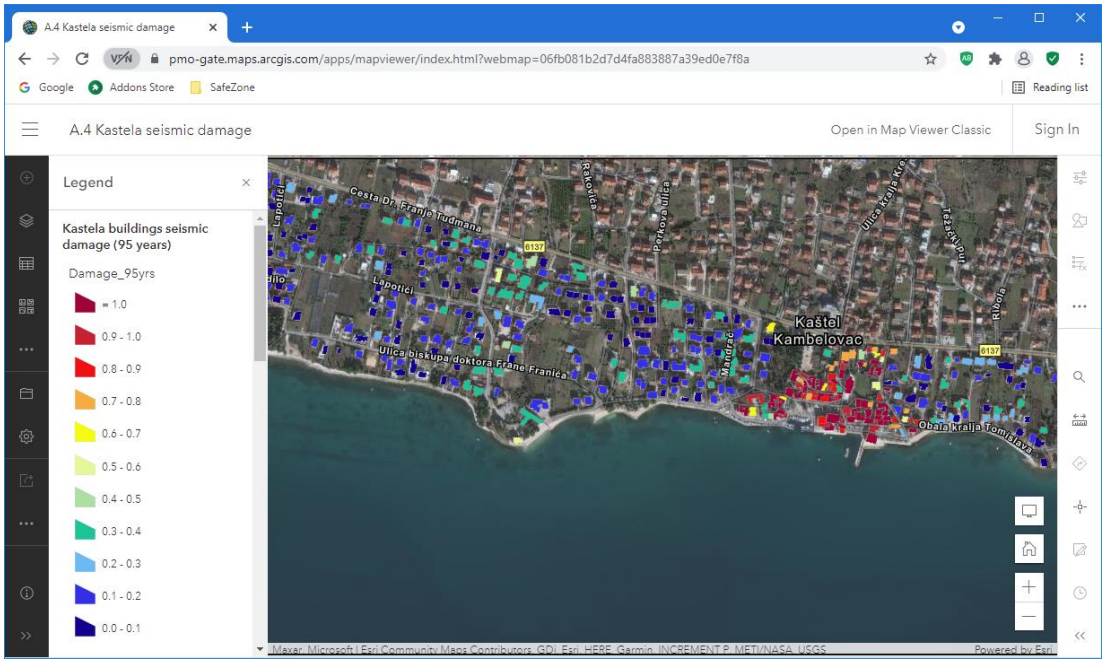

(a) T=95 years

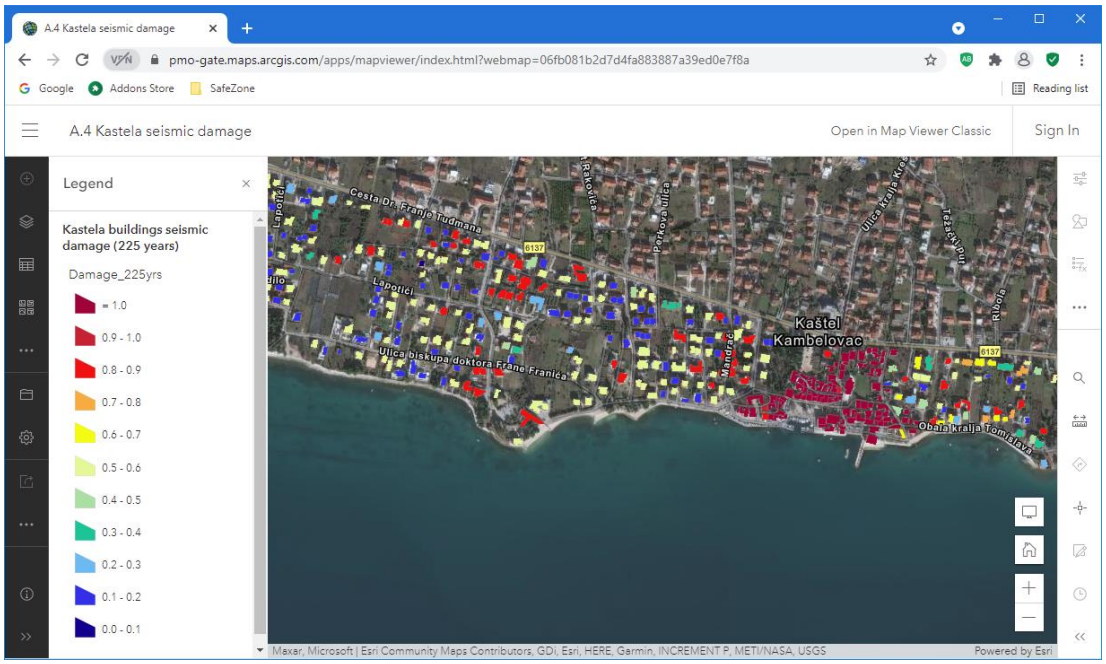

(b) T=225 years

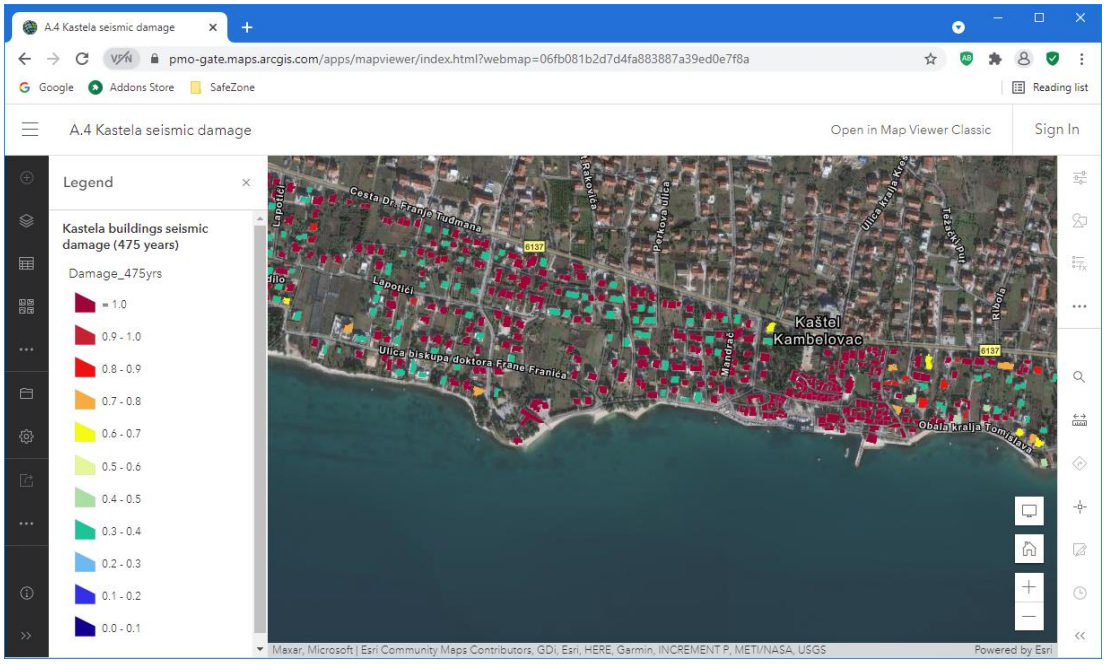

(c) T=475 years

Fig. 16. Damage index maps for different return periods.

4.3.2 Spatial distribution of the seismic risk in terms of peak ground acceleration

Spatial distribution of the seimic risk in terms of index of sesimic risk is represented by the risk maps of the test area for three seismic scenarious represented by return periods of 95, 225 and 475 years, respectively.

Index of seismic risk is defined as a ratio between the peak ground acceleration corresponding to the capacity of the structure PGA_C and the demand ground acceleration according to Deliverables 3.3.1 and 3.3.3. It is expressed in a form:

$$\alpha_{PGA,C} = \frac{PGA_C}{PGA_D} \quad (1)$$

where PGAD represents demand peak ground acceleration for selected return period.

The values $\alpha_{PGA}>1$ are related to safe structures, while the values $\alpha_{PGA}<1$ are related to non-safe structures.

In this project the index of seismic risk for the collapse of the structure which corresponds to the collapse (NC limit state) is estimated for three return periods. The results are presented in Fig. 17.

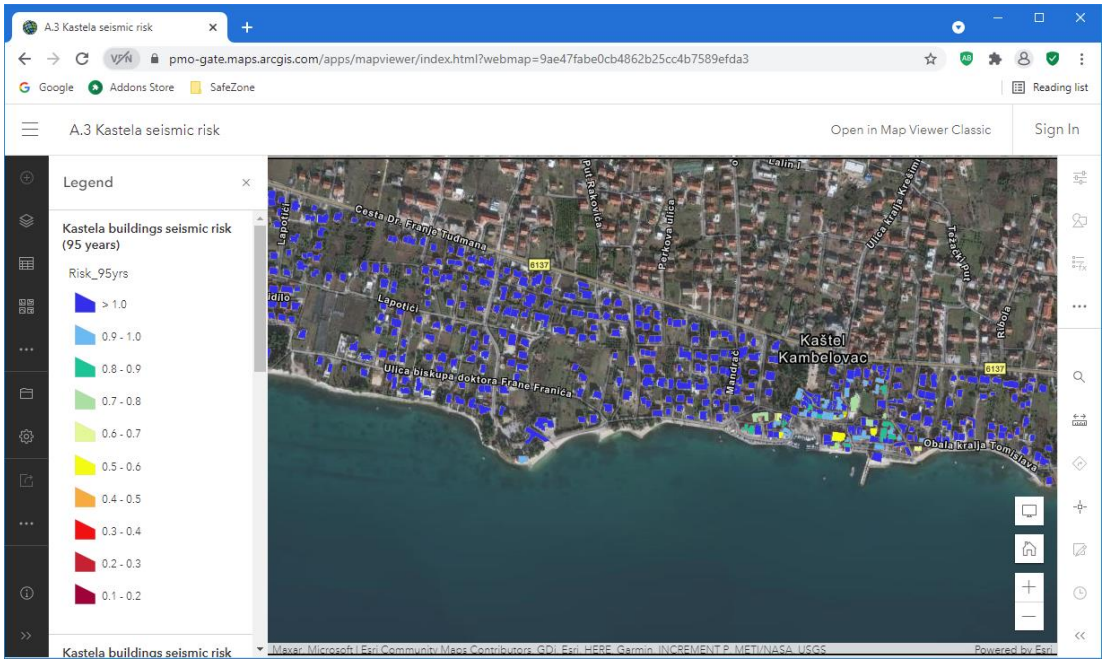

(a) T=95 years

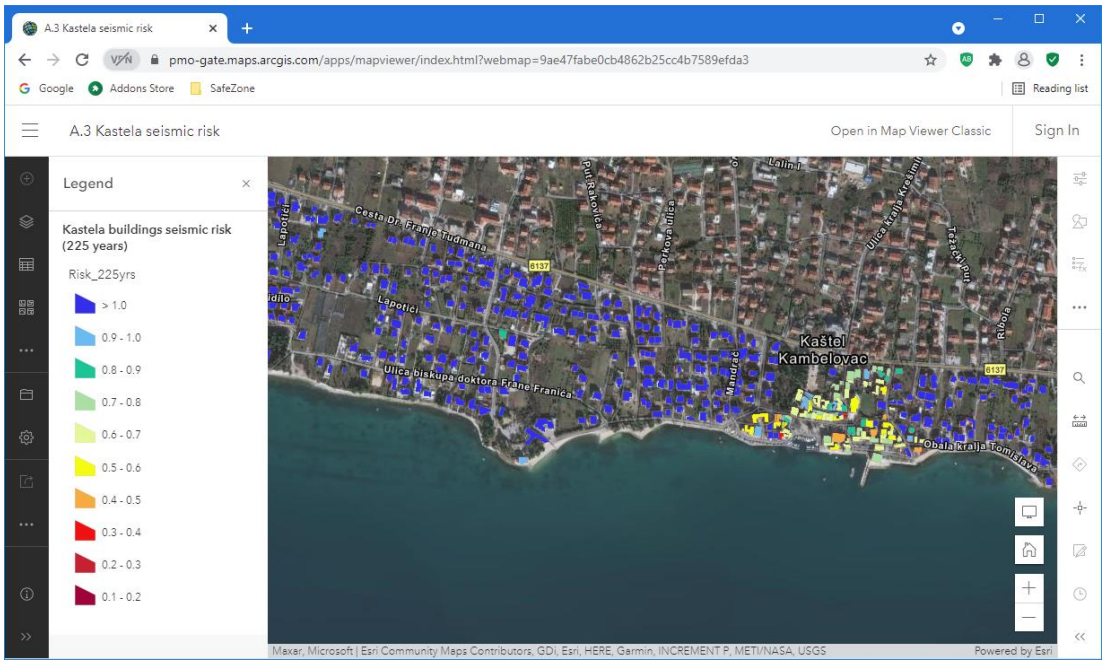

(b) T=225 years

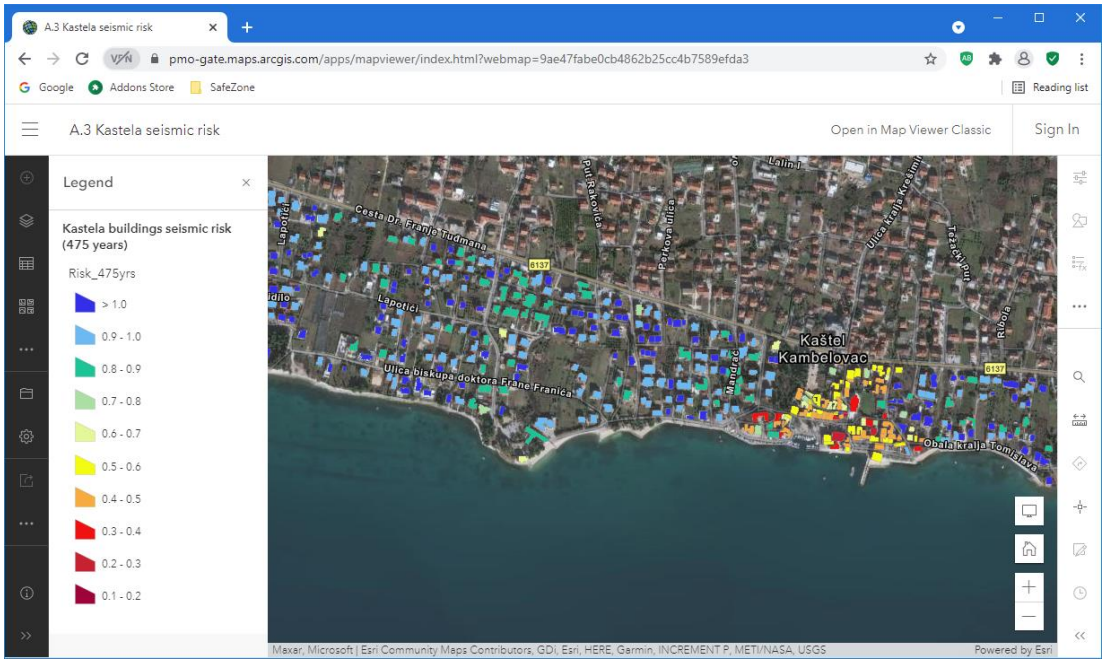

(c) T=475 years

Fig. 17. Risk maps in terms of index of seismic risk for different return periods.

5 Additional functionalities of the Web maps

By clicking on any building in the map, a pop-up window appears with all the attributes (Fig. 18) and a photo of the building is available for all buildings in historical center (Fig. 19).

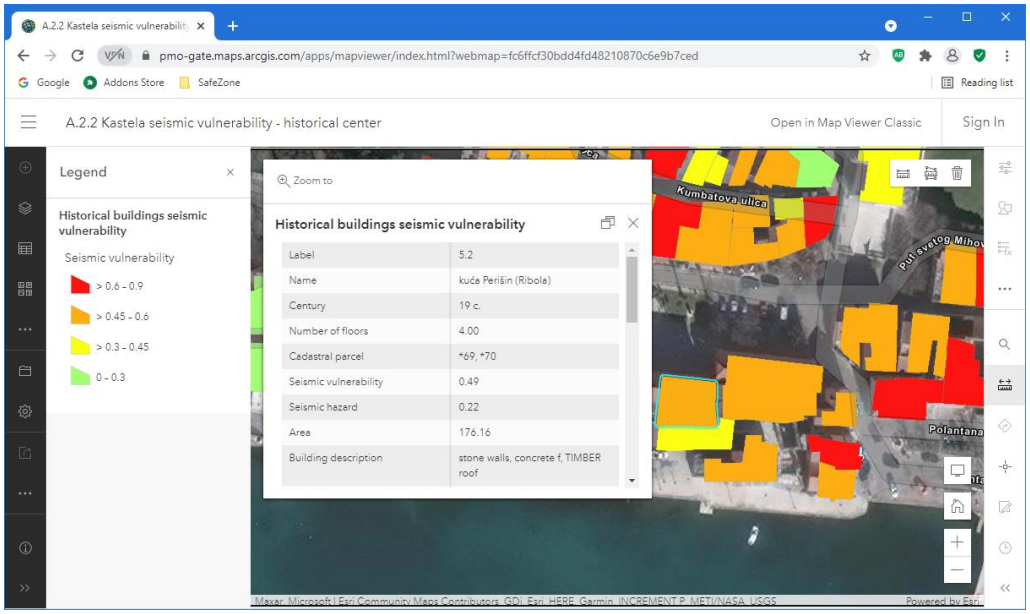

Fig. 18. A pop-up window with building's attributes.

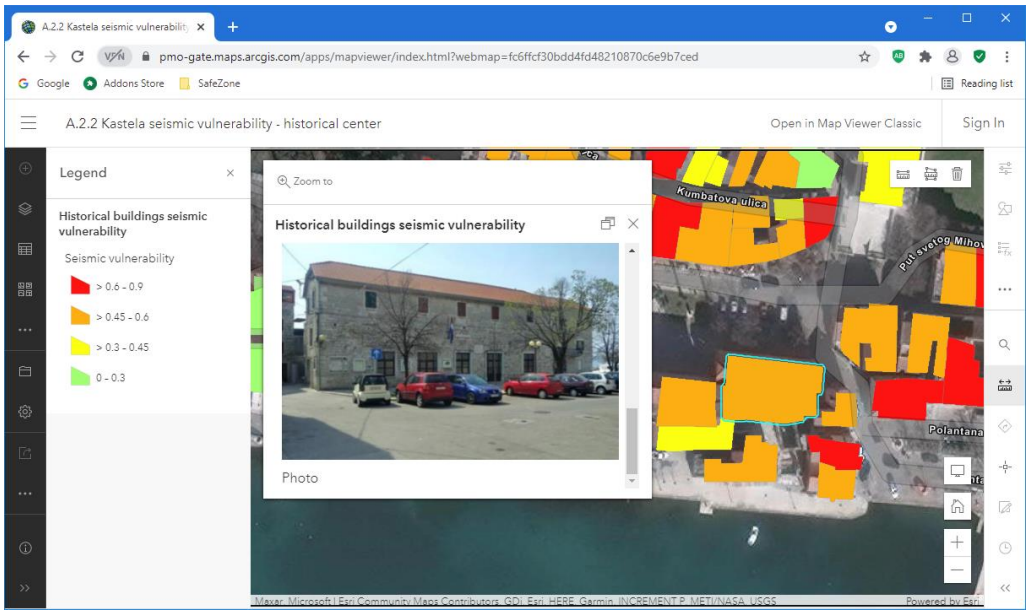

Fig. 19. A pop-up window with building's photo.

Additionally, spatial tools like area measurement can be used with ease to gain some additional information (Fig. 20). A customization of the Web maps is also possible. The basemap of the Web map can be changed from Imagery basemap to Topographic, Streets, or similar basemap. A symbology of the layer can be changed by defining a different style for a layer. Nevertheless, a special effects – bloom, blur, drop shadow, etc. – can be applied to layer to produce more attractive map (Fig. 21).

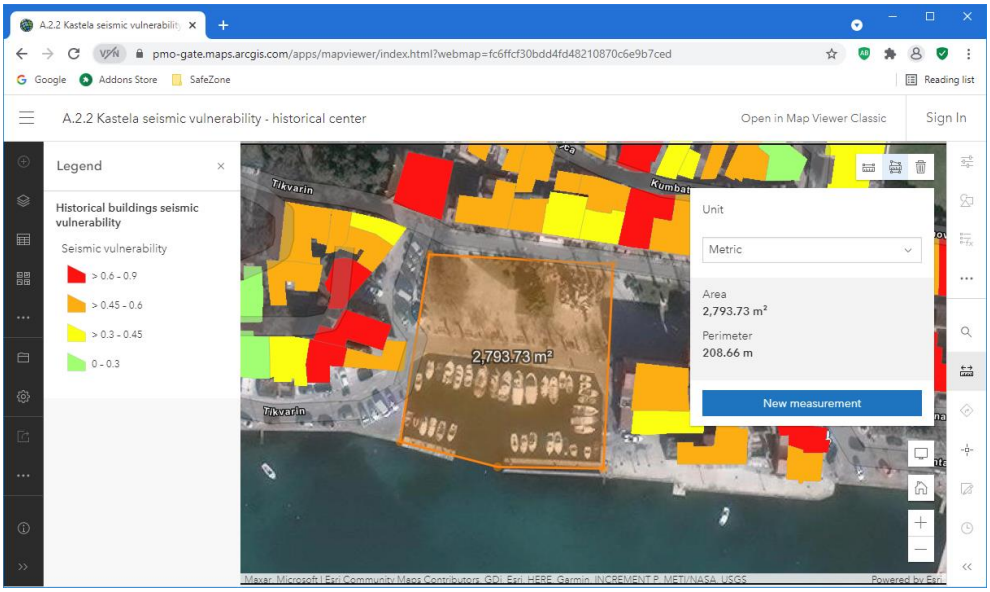

Fig. 20. Line and area measurement tool.

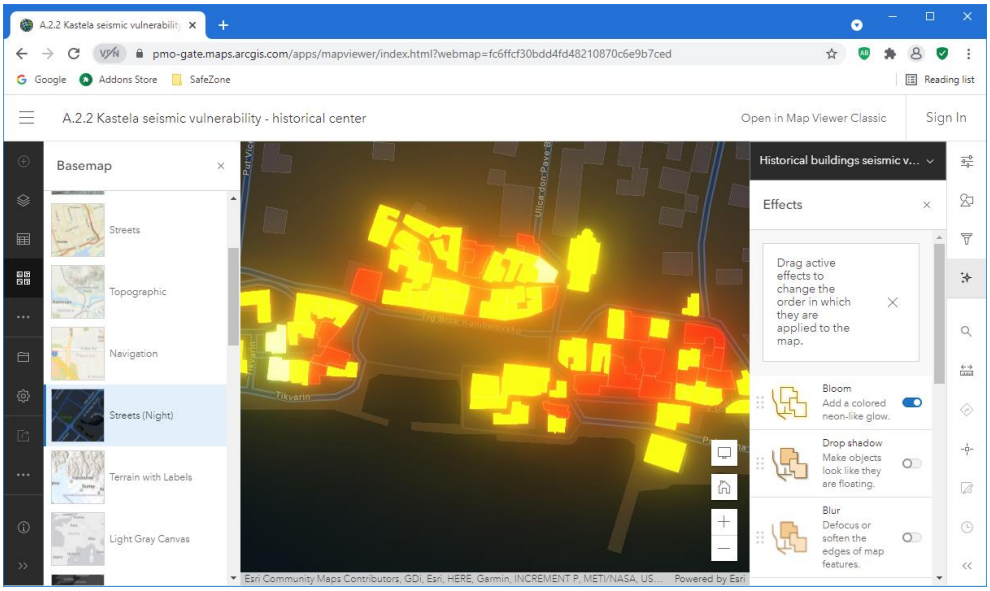

Fig. 21. Applying effect on a layer.

Furghtermore, any additional GIS layer can be added to the Web map for further analysis and especially for the Multi-Hazard Risk Assessment based on Multi-Criteria Analysis.

Conclusions

The maps in this Deliverable are results of inputs from other deliverables, and they are available as Web maps on Web platform that has been established. Main visualization has been made through Geographic Information System (GIS) which succesfully integrated data based on investigations of hazard, vulnerability and risk of the test site to floods, extreme sea waves and earthquakes. The maps enable to identify the buildings and areas with higher risk of natural disasters, which can be a very useful output for urban planning and management purposes. They enable better risk management of HR pilot site Kaštel Kambelovac.

References

[1] Deliverable 3.1.2. Definition of flood exposure indexes for the HR test site, PMO-GATE project, 2021.

[2] Deliverable 3.1.3. Definition of the main weak points of the investigated test sites, PMO-GATE project, 2021.

[3] Deliverable 3.2.1. Definition of meteo-tsunami (extreme sea waves) exposure indexes for the HR test site, PMO-GATE project, 2021.

[4] Deliverable 3.2.2. Definition of the main weak points of the investigated test sites, PMO-GATE project, 2021.

[5] HRN EN 1998-1:2011. Design of structures for earthquake resistance. Part 1: General rules, seismic actions and rules for buildings. Croatian Standards Institute, 2011.

[6] Bohm G, Da Col F, Accaino F, Meneghini F, Schleifer A, Nikolić, Ž. Characterization of shallow sediments in an urban area (Kaštela, Croatia) by analysis of P, SV and Sh seismic velocities using a tomographic approach, Near Surface Geoscience Conference & Exhibition 2020, 30 August - 3 September 2020, Belgrade, Serbia.

[7] Da Col F, Accaino F, Bohm G, MenFeghini F. Characterization of shallow sediments by processing of P, SH and SV wavefields in Kaštela (HR). Engineering Geology 2021, 293, 106336.

[8] Deliverable 3.3.3. Determination of seismic vulnerability indexes for masonry historical buildings located in the HR test site, PMO-GATE project, 2021.

[9] Deliverable 3.3.1. Guidelines of the assessment procedure for earthquake vulnerability in HR test site, PMO-GATE project, 2021.

[10] Deliverable 3.3.4. Seismic vulnerability maps for HR test site, PMO-GATE project, 2021.

[11] Nikolić Ž, Runjić L, Ostojić Škomrlj N, Benvenuti E. Seismic Vulnerability Assessment of Historical Masonry Buildings in Croatian Coastal Area. Applied Sciences, 11, 5997, 2021., https://doi.org/10.3390/app11135997